Liquid Crystals
Publication details, including instructions for authors and subscription information:
http://www.informaworld.com/smpp/title~content=t713926090

Ferroelectric liquid crystals derived from isoleucine II. Orientational ordering by carbon-13 separated local field spectroscopy

Aidi Chen; Chi-Duen Poon; Theo J. Dingemans; Edward T. Samulski

To cite this Article Chen, Aidi , Poon, Chi-Duen , Dingemans, Theo J. and Samulski, Edward T.(1998) 'Ferroelectric liquid crystals derived from isoleucine II. Orientational ordering by carbon-13 separated local field spectroscopy', Liquid Crystals, 24: 2, 255 — 262

To link to this Article: DOI: 10.1080/026782998207433

URL: http://dx.doi.org/10.1080/026782998207433

LIQUID CRYSTALS, 1998, VOL. 24, NO. 2, 255–262

Ferroelectric liquid crystals derived from isoleucine II. Orientational ordering by carbon-13 separated local field spectroscopy

by AIDI CHEN, CHI-DUEN POON, THEO J. DINGEMANS and
EDWARD T. SAMULSKI*

Department of Chemistry, University of North Carolina at Chapel Hill,
Chapel Hill, NC 27599-3290, USA

(*Received 13 May 1997; in final form 5 August 1997; accepted 6 August 1997*)

The orientational ordering of a series of ferroelectric liquid crystals 4′-[(2*S*,3*S*)-3-methyl-2-halopentanoyloxy]-4-hexyloxybiphenyls (3M2**X**PHOB, **X** = **F** for fluorine, **C** for chlorine, **B** for bromine) and their racemates have been studied by two-dimensional carbon-13 separated local field spectroscopy combined with off-magic-angle spinning. All carbons are well-resolved in the carbon-13 NMR spectrum so that carbon–proton dipolar coupling constants for all carbons in the liquid crystal molecule can be determined, giving detailed segmental orientational ordering information. (The order parameters of the biphenyl core segments and each carbon–proton bond in the aliphatic chains were measured as a function of temperature.) The results show that the substitution of different halogens on the chiral chain affects the carbon–proton bond orientational ordering of the entire chiral chain, while the orientational ordering of the rest of the liquid crystal molecule (core and achiral chain) remains unchanged. For the fluoro-substituted liquid crystals, carbon–fluorine dipolar couplings are also observed. At the SmA-to-SmC* transition, there is a discontinuous change in the magnitudes of all C–H bond order parameters. However, the aliphatic ordering relative to the core ordering is unchanged, suggesting that there is a negligible change in the mesogen conformation and the environment of the aliphatic chain at this transition, i.e. there is no evidence for substantial ‘chiral interactions’ in the SmC* phase.

1. Introduction

Ferroelectric liquid crystals (FLCs) have been under active study since their discovery in 1975 [1]. These materials form a chiral smectic C (SmC*) phase which exhibits spontaneous electric polarization; the ultra-fast switching properties of the SmC* phase makes FLCs candidates for the next generation of liquid crystal displays [2]. Hence, considerable effort has been expended on the search for new FLC molecules with large spontaneous polarization. In attempts to enhance the latter property, molecular design has focused on the chiral tail moiety of the FLC [3–5]. Among the most successful building blocks of such chiral tails are the α-halo acids derived from amino acids, e.g. FLCs made from the derivatives of L-isoleucine show large spontaneous polarization [6–8]. In order to understand better the relationship between mesogen molecular structure and FLC attributes, we have prepared a series of liquid crystals derived from L-isoleucine, 4′-[(2*S*,3*S*)-3-methyl-2-halopentanoyloxy]-4-hexyloxybiphenyls (3M2**X**PHOB, **X** = **F** for fluorine, **C** for chlorine, **B** for bromine) and their racemates [9]. These mesogens were studied by a powerful two-dimensional carbon-13 NMR technique which combines separated local field (SLF) spectroscopy with off-magic-angle spinning [10,11]. The SLF NMR technique provides unique conformational insights into these FLCs via the C–H segmental order parameters.

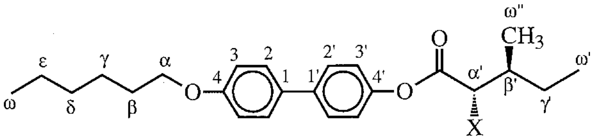

X = fluorine, chlorine and bromine

Macroscopic alignment of the SmA phase along the sample spinning axis (**s**) can be achieved by slow cooling from the isotropic phase in the NMR spectrometer field ($\mathbf{B}_0$) [11]. With about a 1 kHz spinning rate and $B_0 = 7{\cdot}05\,\mathrm{T}$, the SmC* helix is unwound and the aligned 3M2**C**PHOB mesogens behave like a normal monodomain SmC phase [11]. It was reasonable to expect that the fluoro and bromo derivatives of 3M2**X**PHOB would

---

*Author for correspondence.

align like the chloro derivative, and with the local director along **s** these derivatives should exhibit high-resolution carbon-13 spectra. The bromo analogue (3M2**B**PHOB) had been synthesized earlier and shown to be liquid crystalline [12]. The fluoro analogue (3M2**F**PHOB) has not before been reported in the literature.

This work comprises part of a detailed programme wherein we are systematically studying the local segmental orientational ordering in a closely related series of liquid crystals using an improved NMR technique. The 2D SLF NMR experiment provides carbon–proton dipolar coupling constants for each carbon exhibiting a resolved resonance [10]. The resulting local C–H dipolar couplings reveal structural information related to the orientational ordering of each C–H bond (each segment) in the FLC molecule. The large chemical shift range inherent in carbon-13 NMR and the improved resolution by off-magic-angle spinning, enable us to observe details about the orientational ordering of both the aromatic core of the 3M2**X**PHOB mesogen and the C–H bonds in its aliphatic chains. Our goal is to study the order parameters of this series of liquid crystals, which differ from each other by a subtle structural variation (different halogen substitutions), in order to provide data which may lead to a better understanding of the relationship between molecular structure and orientational ordering.

2. Experimental

2.1. *Materials*

The synthesis of 4′-[(2*S*,3*S*)-3-methyl-2-halopentanoyloxy]-4-hexyloxybiphenyls (3M2**X**PHOB, **X** = **F** for fluorine, **C** for chlorine, **B** for bromine) was performed according to procedures described in the literature, with minor modifications [6–8]. The liquid crystalline phases were characterized by differential scanning calorimetry (DSC) and polarizing microscopy. The detailed synthetic procedures, characterization methods, transition temperatures, and measurement of spontaneous polarization are published elsewhere [9].

2.2. *NMR experiments*

All of the NMR experiments were carried out on a Bruker MSL360 NMR spectrometer with a Bruker CP/MAS probe (7 mm rotor). The FLC samples were placed inside a 5 mm glass insert sealed with Kel-F end caps. Temperature calibration was carried out by observing the isotropic to SmA and SmA to SmC* phase transitions.

The carbon–proton coupling constants of FLC samples were measured using the 2D SLF technique [11]. During the t_1 evolution period, proton–proton dipolar couplings were removed by applying a windowless homonuclear dipolar decoupling pulse train (BLEW-48) [13] so that only carbon–proton dipolar couplings were retained. The high resolution carbon-13 spectrum was acquired during the t_2 period with broadband proton decoupling.

In the liquid crystalline phase, the proton–proton dipolar couplings are quite large, hence to obtain first order spectra, very high decoupling power is required to remove them. In turn, this can lead to severe sample heating. To minimize heating and temperature gradient problems, all the experiments were done with the sample spinning at an angle slightly smaller than the magic angle (54·7°). This off-magic-angle spinning technique reduces all the dipolar couplings by a factor of $(3\cos^2\theta\text{-}1)/2$ for liquid crystals with positive diamagnetic anisotropy ($\Delta\chi > 0$), where θ is the angle between the spinning axis (**s**) and the magnetic field ($\mathbf{B}_0$) [14]. When the proper angle θ ($< 54{\cdot}7°$) is chosen, only moderate decoupling power is required to remove the reduced proton–proton dipolar couplings. In our experiments, good resolution at $B_0 = 8{\cdot}46$ T could be achieved in both dimensions with $\theta = 51{\cdot}7°$. At this angle a proton decoupling field of $\gamma B_1/2\pi = 19$ kHz is enough effectively to remove the proton–proton dipolar couplings. A duty cycle of less than 1% was used in order to minimize the effect of radiofrequency heating.

The macroscopic alignment of the local director in the SmA phase could be achieved by cooling the sample slowly from the isotropic phase at spinning rates of 200~400 Hz [11]. After temperature equilibration, the spinning rate was increased to about 1 kHz. For the SmC* phase, the alignment of the molecular director could be achieved by slowly cooling the aligned sample of the SmA phase into the SmC* phase [11]. The observation of sharp carbon-13 peaks was evidence for macroscopic molecular alignment of the SmC* phase.

2.3. *Data processing*

All of the 2D data processing was carried out using FELIX software (Biosym Technologies). The 2D NMR spectra consist of carbon–proton dipolar splitting in the ω_1 dimension and carbon-13 chemical shift in the ω_2 dimension. For each carbon, the dipolar splitting ($\Delta\nu$) was obtained by line-shape fitting on traces from the ω_1 dimension with the FELIX line-shape deconvolution routine. Using these $\Delta\nu$ values, the dipolar coupling constant (D) can be calculated from:

$$\Delta\nu = f\,[(3\cos^2\theta - 1)\,D + J] \qquad (1)$$

where f is a scaling factor characteristic of the dipolar decoupling sequence. For the BLEW-48 homonuclear dipolar decoupling sequence, f equals 0·42 [15]. Because the anisotropic part of the scalar coupling J is very small compared with the dipolar coupling, the isotropic

J values determined in the isotropic solution were used in equation (1).

The biphenyl rings of the FLC molecule 3M2**X**PHOB have effective D_2 symmetry. Therefore, the dipolar coupling constant for each C–H pair is given by:

$$D_{\mathrm{CH}} = -\frac{\gamma_{\mathrm{C}}\gamma_{\mathrm{H}}h}{8\pi^2 r_{\mathrm{CH}}^3}[(3\cos^2\theta_{\mathrm{CH}z}-1)S_{zz} + (\cos^2\theta_{\mathrm{CH}x}-\cos^2\theta_{\mathrm{CH}y})(S_{xx}-S_{yy})] \qquad (2)$$

where γ_{C} and γ_{H} are gyromagnetic ratios for carbon and proton, respectively, h is Planck's constant, r_{CH} is the internuclear distance between the carbon and proton, and $\theta_{\mathrm{CH}\alpha}$ is the angle between r_{CH} and the molecular fixed α-axis. In our molecular fixed frame, **z** is the twofold axis of the phenyl ring and **x** is chosen to lie in the ring plane perpendicular to **z**. In the calculation, it was assumed that the benzene rings have hexagonal symmetry with $r_{\mathrm{CC}}=1\cdot40$ Å and $r_{\mathrm{CH}}=1\cdot08$ Å. The order parameters of the biphenyl core of the molecule (S_{zz}, $S_{xx}-S_{yy}$) and angles $\theta_{\mathrm{CH}\alpha}$ can be obtained by least square fits of the calculated aromatic carbon–proton dipolar coupling constants to the experimental data.

The alkyl chains populate a large number of conformers and it is difficult to simply interpret the D_{CH} values in terms of local conformational preferences [16]. However, the C–H bond orientational order parameters can be obtained for each CH, $\mathrm{CH_2}$, and (axially symmetrical) $\mathrm{CH_3}$ group according to:

$$S_{\mathrm{CH}} = -\frac{4\pi^2 r^3 D_{\mathrm{CH}}}{\gamma_{\mathrm{C}}\gamma_{\mathrm{H}}h} = -4\cdot407\times10^{-5}\,D_{\mathrm{CH}} \qquad (3)$$

where $r=1\cdot10$ Å.

3. Results and discussion

3.1. *3M2***C***PHOB*

Among all the FLCs studied, optically active 3M2**C**PHOB exhibits the largest temperature ranges for the SmA and SmC* phases. It has been previously shown that the SmA and SmC* phases of 3M2**C**PHOB give high-resolution carbon-13 spectra ($B_0=7\cdot05$ T and $\theta=47\cdot8°$ with spinning rate ~1 kHz) [11]. We have found that macroscopic alignment can also be achieved at $B_0=8\cdot46$ T and $\theta=51\cdot7°$ with a spinning rate of ~1 kHz. Unlike the previous results (where the peaks for carbon 2 and 2′, γ and γ′ were overlapped) [11], all carbon peaks are resolved under our experimental conditions and thus more information with better accuracy is obtained. The results in the present study are consistent with previous work.

Figure 1 shows the order parameters, S_{CH} and S'_{CH}, measured for the achiral and chiral aliphatic C–H bonds respectively, and S_{zz} and S'_{zz} for the two corresponding phenyl rings as a function of temperature (the prime signifies the chiral end of the mesogen). The calculated values of S_{zz} and S'_{zz} are the same within experimental error, which indicates that the C_2 axes of the two phenyl rings are collinear as expected. The biaxial order parameters ($S_{xx}-S_{yy}$) and ($S'_{xx}-S'_{yy}$) (not shown in figure 1) are around zero indicating a nearly uniaxial mesogenic core. The dashed lines show the core order parameters, S_{zz} and S'_{zz}, determined from chemical shifts of $\mathrm{C_3}$ and $\mathrm{C'_3}$ atoms on each ring. Within the experimental uncertainty, S_{zz} and S'_{zz} values obtained from chemical shift data and those from the dipolar couplings are the same. On cooling from the SmA to SmC* phase, S_{zz} and S'_{zz} clearly show a discontinuity at this first order phase transition [17].

In order to explore the conformational changes at the SmA to SmC* phase transition, the reduced order parameters of the aliphatic chains (the S_{CH} values are normalized by the order parameter of the aromatic core S_{zz}) are examined. As can be seen from figure 2 the ratio S_{CH}/S_{zz} displays almost no temperature dependence within experimental error and no visible jump at the SmA to SmC* phase transition. This suggests that the conformer population of aliphatic chains does not change, or alternatively that there is a minimal change in the chain's local environment at the (normal) SmA to (tilted) SmC* transition.

3.2. *3M2***B***PHOB*

The optically active 3M2**B**PHOB shows both SmA and SmC* phases by DSC and optical microscopy measurements. The ring and aliphatic C–H order parameters of the optically active 3M2**B**PHOB in its SmA phase are shown in figure 3. The data show that the two phenyl rings are collinear ($S_{zz}\approx S'_{zz}$) and uniaxial ($S_{xx}-S_{yy}\approx S'_{xx}-S'_{yy}\approx 0$) in this FLC also. The S_{zz} and S'_{zz} of 3M2**B**PHOB are essentially the same as the values determined for 3M2**C**PHOB. Unfortunately, the SmC* phase of 3M2**B**PHOB has only a ~1° temperature range and the temperature gradient in our MAS probe exceeds this. Hence, we could not observe a carbon-13 spectrum in the SmC* phase. In an attempt to circumvent this problem, we synthesized the racemate of 3M2**B**PHOB from *allo*-isoleucine, a mesogen composed of four stereoisomers that constitute two mirror image pairs: [(2*S*,3*S*), (2*R*,3*R*)], and [(2*S*,3*R*), (2*R*,3*S*)]. The labels 2 and 3 correspond to the α′ and β′ carbons respectively in the chiral chain of 3M2**X**PHOB. It was anticipated that the SmC* phase temperature range would be larger in the mixture of diastereomers. Indeed, the SmC* phase temperature range for the racemate of 3M2**B**PHOB was determined to be ~6° [12].

The carbon-13 spectrum of the racemate of 3M2**B**PHOB shows extra peaks relative to the optically active (2*S*,3*S*) sample. These extra peaks are due to the

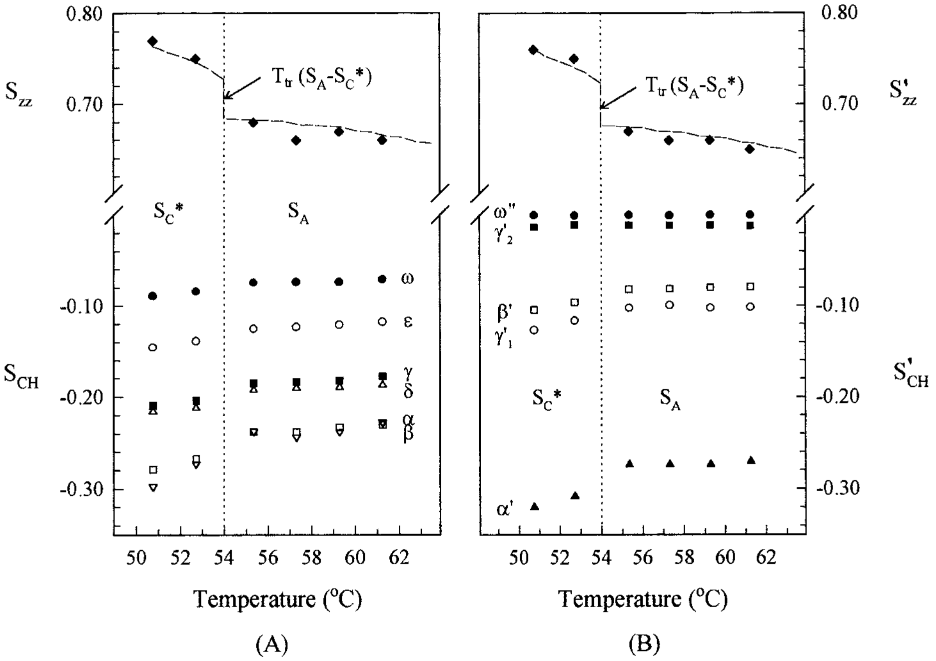

Figure 1. Order parameters of optically active 3M2CPHOB as a function of temperature; the uncertainties are about 10%. The dotted line indicates the transition temperature from SmA to SmC* phase. (*a*) S_{CH} for the *n*-hexyl chain and S_{zz} for the phenyl ring connected to the *n*-hexyl chain. (*b*) S'_{CH}, for the chiral chain and S'_{zz} for the phenyl ring connected to the chiral chain. The dashed lines show the core order parameters determined from chemical shifts of C_3 and C'_3 atoms.

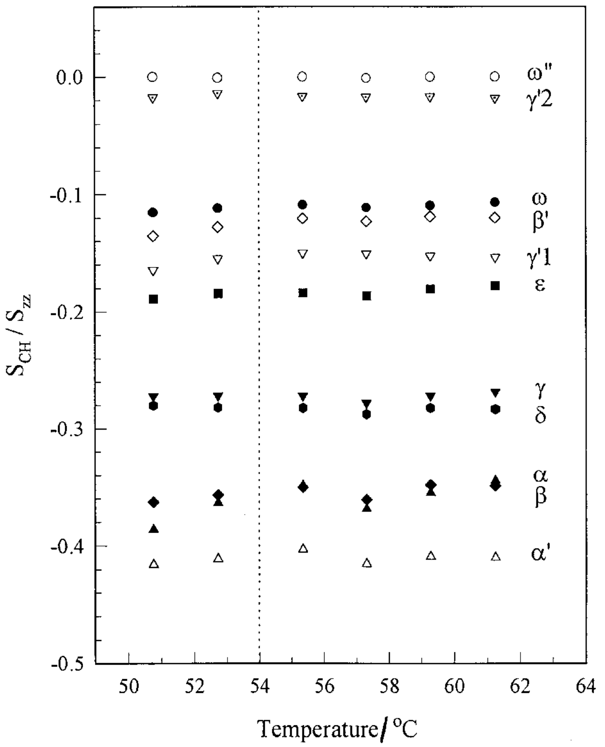

Figure 2. Normalized C–H bond order parameter (S_{CH}/S_{zz}) for optically active 3M2CPHOB along the aliphatic chains, as a function of temperature. The dotted line indicates the transition temperature from SmA to SmC* phase.

stereoisomers [(2*S*,3*R*) and (2*R*,3*S*)]; and are highlighted with circles in figure 4. The mirror image stereoisomers [(2*S*,3*S*) and (2*R*,3*R*)] exhibit the same chemical shifts (and carbon–proton dipolar couplings), as do the stereoisomers [(2*S*,3*R*) and (2*R*,3*S*)]. Under our experimental conditions, carbon peaks on the chiral chain of the [(2*S*,3*S*) and (2*R*,3*R*)] pair of stereoisomers are well-separated from those of the [(2*S*,3*R*) and (2*R*,3*S*)] pair with the exception of the β′ carbon. This observation allows us to study the orientational ordering of different stereoisomers in the diastereomeric mixture. It is interesting to observe that the [(2*S*,3*S*) and (2*R*,3*R*)] stereoisomers and [(2*S*,3*R*) and (2*R*,3*S*)] stereoisomers exhibit quite different dipolar splittings, as shown in figures 5 (*a*) and 5 (*b*). This implies that the orientational ordering (conformational averaging) of the C–H bonds in the chiral chain of these two sets of stereoisomers is quite different. Furthermore, the [(2*S*,3*S*) and (2*R*,3*R*)] set in the racemate gives dipolar splittings similar to those found in the optically pure (2*S*,3*S*) 3M2**B**PHOB [compare figure 5 (*b*) with 5 (*c*)]. This latter result indicates that the C–H bond orientation ordering of the chiral chain in the (2*S*,3*S*) isomer does not change significantly upon dilution with other stereoisomers in the SmA phase. This observation implies that the S'_{CH} order parameters are determined primarily by intramolecular (isomerizational) considerations.

The alignment of the spinning racemate of 3M2**B**PHOB showed unusual behaviour. Upon slow cooling from the isotropic to SmA phase, sharp carbon-13 peaks were observed, indicative of excellent macroscopic alignment. However, the spectral quality deteriorated

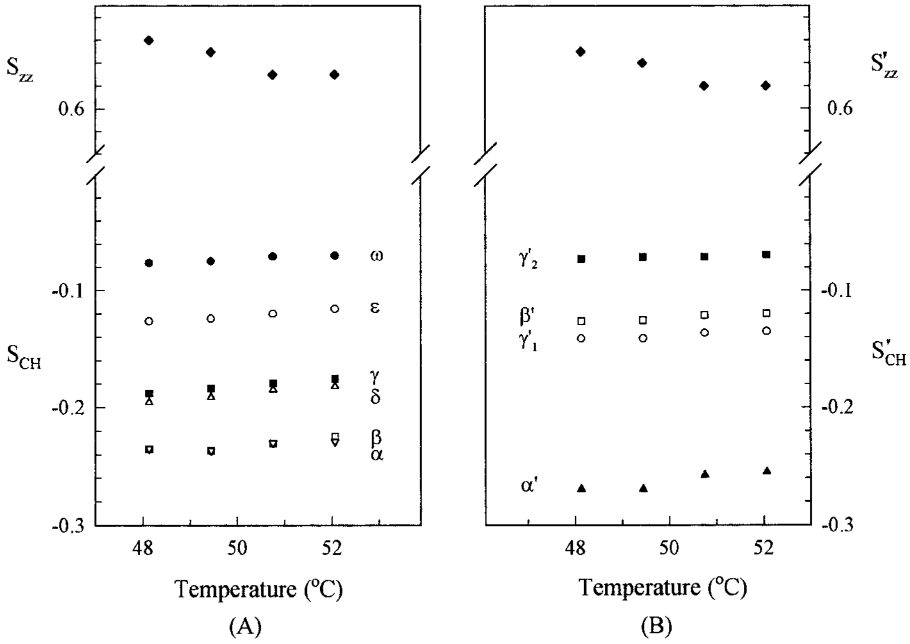

Figure 3. Order parameters of the racemate of 3M2**B**PHOB in its SmA phase, as a function of temperature; the uncertainties are about 10%. (*a*) S_{CH} for the *n*-hexyl chain and S_{zz} for the phenyl ring connected to the *n*-hexyl chain; (*b*) S'_{CH} for the chiral chain and S'_{zz} for the phenyl ring connected to the chiral chain.

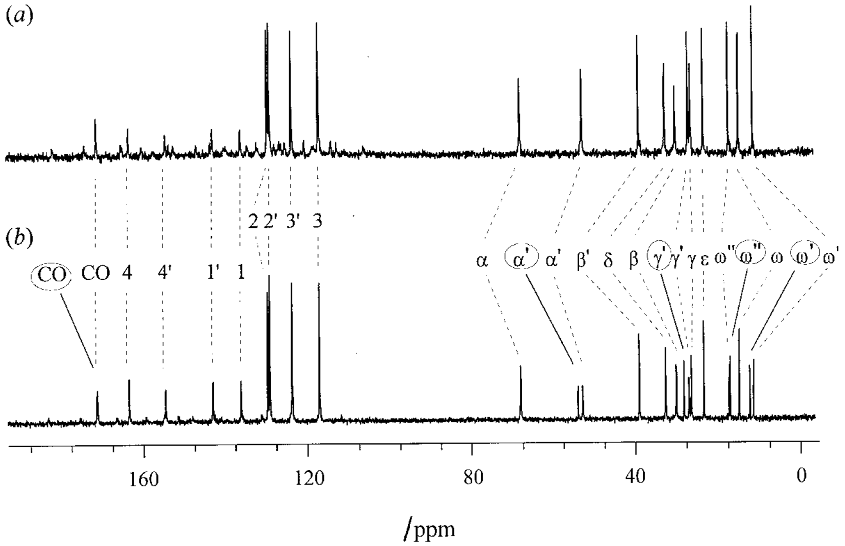

Figure 4. Carbon-13 spectra of (*a*) optically active 3M2**B**PHOB (*b*) the racemate of 3M2**B**PHOB in their SmA phases at 3 K below the isotropic transition temperature.

with time: a partial powder pattern developed after ~10 h. By comparison, the alignment of optically active (2*S*,3*S*) 3M2**B**PHOB did not show any changes with time. One possible explanation of the spectral degradation over time is the occurrence of microphase separation of the different stereoisomers to form distinct (liquid) crystals of the components of the racemic mixture, which in turn disrupts the long range alignment of the sample. Additionally, sample alignment could not be achieved when the (aligned) SmA phase was allowed to cool down into the SmC* phase (a partial powder spectrum is observed). As a result, the orientational ordering of the racemate of 3M2**B**PHOB in its SmC* phase could not be studied.

3.3. *3M2*F*PHOB*

For optically active 3M2**F**PHOB, the SmA phase temperature range is very narrow (~1·5°) and it is very difficult to observe a carbon-13 spectrum of the neat SmA phase. The SLF experiment can be carried out in a two-phase sample having both SmA and isotropic phases present in the experimental temperature gradient. However, serious peak overlap precludes the determination of the orientational ordering of the phenyl ring connected to the chiral chain (S'_{zz}). Also, the C–H dipolar coupling for the ω′ carbon is not resolved. S_{zz} and aliphatic S_{CH}s can be determined (the table); moreover, the presence of a fluorine spin-1/2 nucleus in the molecule gives the possibility for a more detailed structural

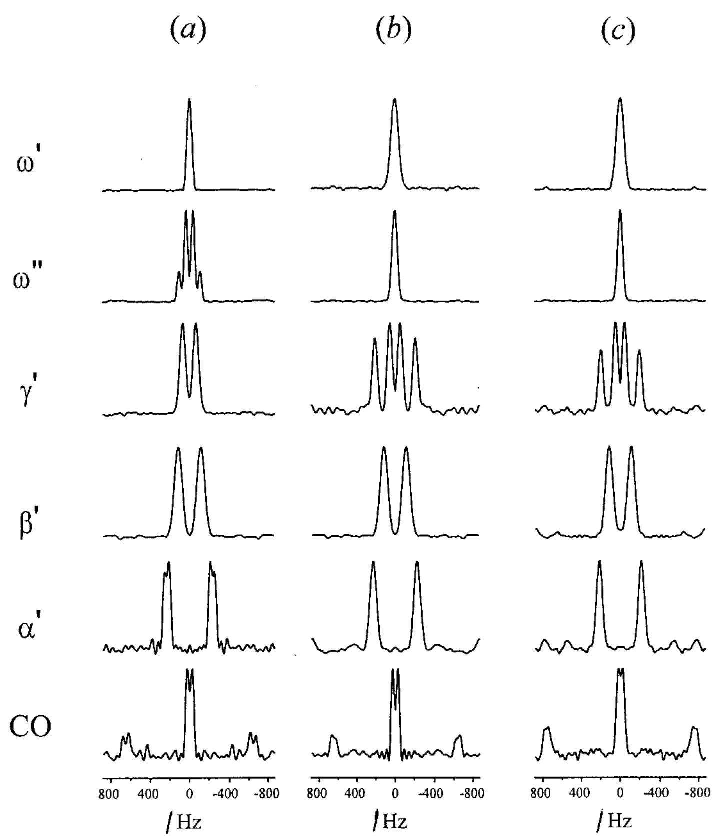

Figure 5. Dipolar splittings of each C–H bond along the chiral chain. (*a*) [(2*S*,3*R*) and (2*R*,3*S*)] components in the racemate of 3M2**B**PHOB, their carbon-13 chemical shift is highlighted with a circle in figure 4; (*b*) [(2*S*,3*S*) and (2*R*,3*R*)] pair in the racemate of 3M2**B**PHOB; (*c*) Optically active 3M2**B**PHOB.

Table 1. Order parameters of the optically active form and the racemate of 3M2**F**PHOB at 81°C in the SmA phase. Some of the order parameters are not available (as indicated by N/A) due to peak overlapping in the ω_1 dimension. The C–H dipolar splittings for ω′ carbon and ω″ carbon of the [(2*S*,3*R*) and (2*R*,3*S*)] pair in the racemate are unresolved in the ω_2 dimension.

		Racemate of 3M2**F**PHOB	
S	3M2**F**PHOB (2*S*,3*S*)	(2*S*,3*S*) & (2*R*,3*R*)	(2*S*,3*R*) & (2*R*,3*S*)
α′	−0·29	−0·29	−0·27
β′	−0·04	−0·05	−0·05
γ′	−0·03	−0·03	N/A
ω′	unresolved	unresolved	
ω″	−0·03	−0·03	unresolved
α	−0·25	−0·24	
β	−0·24	−0·24	
γ	−0·19	−0·18	
δ	−0·18	−0·19	
ε	−0·12	−0·11	
ω	−0·07	−0·07	
S_{zz}	−0·65	0·66	
S'_{zz}	N/A	0·66	

analysis from the dipolar coupling between carbon-13 and fluorine-19. The C–F dipolar coupling constant can be determined not only for one bond C–F coupling as for protons, but also for long range (up to three bond) C···F couplings. In the case of optically active 3M2**F**PHOB, the $D(\mathrm{C}_{\alpha'}\text{–F})$ and $D(\mathrm{C}_{\beta'}\cdots\mathrm{F})$ are found to be 2·0 and 0·62 kHz, respectively.

The narrow temperature range of the SmA phase in the optically active 3M2**F**PHOB forced us to study the racemate of 3M2**F**PHOB for the same reason as for 3M2**B**PHOB. In the diastereomeric mixture, there are the aforementioned 'extra peaks' for the chiral chain. Furthermore, due to carbon–fluorine coupling, more peaks are observed and peak overlap resulted {i.e. the γ and γ′ carbons from [(2*S*,3*R*) and (2*R*,3*S*)] stereoisomers}. The S_{CH} value for the ω′ carbon of all isomers and the ω″ carbon of the [(2*S*,3*S*) and (2*R*,3*R*)] pair are not resolved. The observed order parameters are shown in the table. The $D(\mathrm{C}_{\alpha'}\text{–F})$, $D(\mathrm{C}_{\beta'}\cdots\mathrm{F})$, $D(\mathrm{C}_{\gamma'}\cdots\mathrm{F})$, $D(\mathrm{C}_{\omega''}\cdots\mathrm{F})$ for the [(2*S*,3*S*) and (2*R*,3*R*)] stereoisomers are found to be 2·1, 0·63, 0·14 and 0·12 kHz, respectively. The $D(\mathrm{C}_{\alpha'}\text{–F})$, $D(\mathrm{C}_{\beta'}\cdots\mathrm{F})$, $D(\mathrm{C}_{\omega''}\cdots\mathrm{F})$ for the [(2*S*,3*R*) and (2*R*,3*S*)] stereoisomers are found to be 2·2, 0·63 and 0·3 kHz, respectively. The $D(\mathrm{C}_{\gamma'}\cdots\mathrm{F})$ can not be determined due to peak overlapping.

For 3M2**F**PHOB similar conclusions can be drawn as for the other two FLCs: (a) the stereoisomer pairs with different chemical shifts show different order parameters; (b) the mixing of the stereoisomers does not seem to change the average conformation relative to the pure isomer; (c) despite the differences in the chiral chain, the stereoisomers of 3M2**F**PHOB in the racemate give the same order parameter for both the aromatic core and the *n*-hexyl chain; (d) the order parameters (S_{zz} and S'_{zz}) for the two phenyl rings are essentially the same within experimental error; and finally (*e*) $S_{xx} - S_{yy} \approx S'_{xx} - S'_{yy} \approx 0$.

3.4. *Comparison of 3M2***C***PHOB, 3M2***B***PHOB and 3M2***F***PHOB*

Due to the difficulty in getting information in the SmC* phase for 3M2**B**PHOB and the lack of a SmC* phase in 3M2**F**PHOB, we can only compare the orientational ordering in the SmA phases. However in the case of 3M2**C**PHOB, we note there is no significant change of local environment (C–H averaging by isomerization) as the phase changes from SmA to SmC*. It is interesting to observe that the orientational ordering of the aromatic cores and the *n*-hexyl chains are very similar in all three FLCs. At the same time, the dipolar couplings along the chiral chain show clear differences as the size of **X** increases from fluorine to chlorine to bromine, as shown in figure 6. So the variation of halogen substitution on the α′ carbon changes the orientational ordering of the whole chiral chain as a result of changes in local conformational preferences without altering the ordering of the rest of the molecule.

4. Conclusions

The liquid crystals 3M2**F**PHOB, 3M2**C**PHOB, 3M2**B**PHOB, and their racemates were studied by the 2D SLF NMR technique. Orientational ordering information on the mesogen biphenyl core segment and each C–H bond of the aliphatic chains was determined as a function of temperature. The reduced order parameters (S_{CH}/S_{zz} values) of each C–H bond for the optically active 3M2**C**PHOB display little temperature dependence, within experimental error, even at the phase transition temperature. This unequivocally indicates that there is no packing-induced conformational transformation in either the chiral or achiral chain on going from the normal SmA to tilted SmC* phase, i.e. local intermolecular interactions in the aliphatic component of the stratified smectics do not change significantly at the SmA to SmC* transition. This may imply that the SmA to SmC* transition is driven by satisfying rather general excluded volume and/or electrostatic interactions between the (average) mesogens.

The study of the racemates indicates that the mixing of the stereoisomers does not change the orientational ordering from that found in the pure isomer. This observation further supports the idea that intramolecular constraints dominate the observed C–H ordering, independent of changes in the mesogen environment that accompany dilution (racemic mixtures) or tilting (SmA to SmC* transition). These findings argue against any substantial 'chiral interactions' in the SmC* phase— there is no evidence for the appearance of a new interaction in the chiral phase which could alter the conformational preferences of the mesogens.

Despite the different halogen substitution at the α′ carbon of these FLCs and the different configurations of the two chiral centres for the stereoisomers, the aromatic cores and the achiral aliphatic chain exhibit quite similar order parameters. Consequently, the

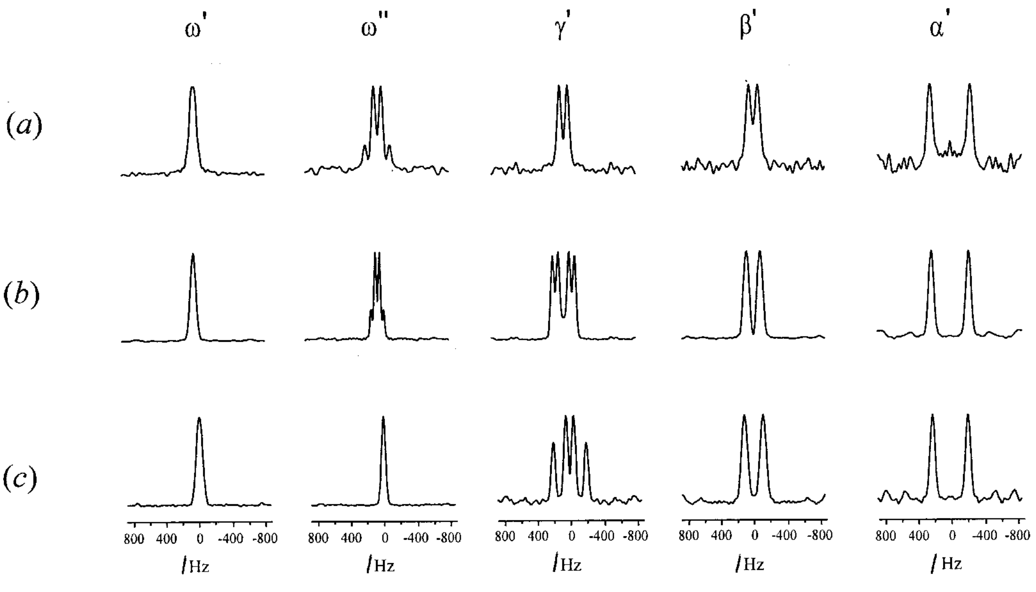

Figure 6. Dipolar splittings of the C–H bond of the chiral chain in SmA phases. (*a*) 3M2**F**PHOB, (*b*) 3M2**C**PHOB, (*c*) 3M2**B**PHOB, at 1 K, 3 K and 3 K below isotropic transition temperature, respectively.

changes produced in the chiral chain on substituting the halogens are very localized. On the other hand, the local substitution at the α' carbon of these FLCs changes the order parameters of every carbon–proton bond on the chiral chain, indicating that this substitution substantially changes the conformational averaging in the chiral chain.

This work was supported by NSF grant DMR-941271.

References

[1] Meyer, R. B., Liébert, L., Strzelecki, L., and Keller, P., 1975, *J. Physique (Lett.)*, **36,** L69.

[2] Lagerwall, S. T., 1996, *Liq. Cryst. Today*, **6,** 5.

[3] Walba, D. M., Slater, S. C., Thurmes, W. N., Clark, N. A., Handschy, M. A., and Supon, F., 1986, *J. Am. chem. Soc.*, **108,** 5210.

[4] Koden, M., Kuratate, T., Funada, F., Awane, K., Sakaguchi, K., and Shiomi, Y., 1990, *Mol. Cryst. liq. Cryst. Lett.*, **7,** 79.

[5] Photinos, D. J., and Samulski, E. T., 1995, *Science*, **270,** 783.

[6] Sakurai, T., Mikami, N., Higuchi, R., Honma, M., Ozaki, M., and Yoshino, K., 1986, *J. chem. Soc., chem. Comm.*, 978.

[7] Bahr, Ch., and Heppke, G., 1986, *Mol. Cryst. liq. Cryst. Lett.*, **4,** 31.

[8] Sierra, T., Serrano, J. L., Ros, M. B., Ezcurra, A., and Zubia, J., 1992, *J. Am. chem. Soc.*, **114,** 7645.

[9] Dingemans, T. J., Poon, C.-D., Samulski, E. T., Uehara, H., and Hatano, J., 1998, *Liq. Cryst.*, **24** (2), 247.

[10] Fung, B. M., and Afzal, J., 1986, *J. Am. chem. Soc.*, **108,** 1107.

[11] Poon, C.-D., and Fung, B. M., 1989, *J. chem. Phys.*, **91,** 7392.

[12] Ozaki, M., Yoshino, K., Sakurai, T., Mikami, N., and Higuchi, R.-I., 1987, *J. chem. Phys.*, **86,** 3648.

[13] Burum, D. P., Linder, M., and Ernst, R. R., 1981, *J. Magn. Reson.*, **44,** 173.

[14] Courtieu, J., Alderman, D. W., and Grant, D. M., 1981, *J. Am. chem. Soc.*, **103,** 6783.

[15] Fung, B. M., 1987, *J. Magn. Reson.*, **72,** 353.

[16] Photinos, D. J., Samulski, E. T., and Toriumi, H., 1991, *J. chem. Phys.*, **94,** 2758.

[17] Bräuniger, T., and Fung, B. M., 1995, *J. Chem. Phys.*, **102,** 7714.